# Enhanced Receiver Based on FEC Code Constraints for Uplink NOMA With Imperfect CSI

Pei-Rong Li, Zhi Ding<sup>®</sup>, Fellow, IEEE, and Kai-Ten Feng<sup>®</sup>, Senior Member, IEEE

Abstract—Non-orthogonal multiple access (NOMA) has been envisioned as a useful component of fifth generation (5G) mobile networks. As imperfect channel state information (CSI) due to channel estimation errors poses problems for most wireless receivers, it presents even greater challenges in successive interference cancellation (SIC) reception of NOMA signals. We present a novel approach to the multi-user detection problem by exploiting the important constraints of forward error correction (FEC) code word. We devise our new receiver based on the minimum output energy (MOE) criterion while preserving a distortionless response to the user equipment (UE) of interest. In particular, we efficiently adopt the UE signatures presented by the FEC channel codes under distinct permutations to separate desired signals of interest from interfering UEs. We formulate our receiver optimization into a quadraticprogramming problem anchored with a set of code constraints. Our simulations demonstrate that the proposed code-anchored quadratic programming (CQP) receiver can accurately improve SIC performance and provide robustness to CSI errors better than other legacy schemes.

Index Terms—NOMA, FEC code signature, code-anchored quadratic programming (CQP).

#### I. INTRODUCTION

N AN era of rapid growth for mobile internet, spectral efficiency is viewed as one of the key concern in an effort to accommodate such huge volumes of data traffics. A number of effective solutions as well as potential candidates have been proposed to further enhance system capacity in the emerging versions of the fifth generation (5G) cellular standard released by the 3GPP [1], [2]. Non-orthogonal multiple access (NOMA) has been recently identified as a promising cooperative transmission technology that is expected to find applications in deployment of the 5G networks [2]–[4]. NOMA involves the effective sharing of radio resources

Manuscript received November 11, 2018; revised April 22, 2019; accepted July 1, 2019. Date of publication July 24, 2019; date of current version October 9, 2019. The work of P.-R. Li and K.-T. Feng was supported in part by the Ministry of Science and Technology (MOST) under Grant 107-2622-8-009-020, Grant 107-2218-E-009-047, and Grant 107-2221-E-009-058-MY3. The work of Z. Ding was supported by the National Science Foundation under Grant 1711823. The associate editor coordinating the review of this paper and approving it for publication was Z. Zhang. (corresponding author: Kai-Ten Feng.)

P.-R. Li and K.-T. Feng are with the Department of Electrical and Computer Engineering, National Chiao Tung University, Hsinchu 300-10, Taiwan (e-mail: shockbowwow.cm01g@nctu.edu.tw; ktfeng@mail.nctu.edu.tw).

Z. Ding is with the Department of Electrical and Computer Engineering, University of California at Davis, Davis, CA 95616 USA (e-mail: zding@ucdavis.edu).

Color versions of one or more of the figures in this article are available online at http://ieeexplore.ieee.org.

Digital Object Identifier 10.1109/TWC.2019.2929386

among user equipments (UEs) in a given scenario. Different from conventional approach of orthogonal resource allocation among different UEs in various combinations of frequency, time, or code domains, NOMA allows UEs to share the same resource in a non-orthogonal manner. In particular, the ongoing studies toward NOMA in the form of multi-user superposition transmission (MUST) have attracted substantial attention by increasing network throughput and improving connectivity for future wireless communication systems. MUST is a special case of NOMA in which multipexing of UE's signal is operated in power domain. To combat inter-user interference, successive interference cancellation (SIC) is performed at receivers to decode a superimposed signal with a specific order of channel gains [4].

Despite a number of practical advantages, the benefits of NOMA systems are limited by several physical factors. The prevailing design of SIC receivers requires high channel gain disparity to ensure the applicability of NOMA [5]. Namely, a UE with weak channel gain is squeezed into a channel occupied by a UE with a stronger channel gain. Accurate channel state information (CSI) is essential to avoid error propagation in SIC receivers. Most existing works on NOMA have relied on the perfect CSI assumption [6], [7], which is difficult to realize in practice. The reason is that long pilot signals sent to enhance estimation accuracy of CSI imposes significant system overhead that ironically would lower the spectral efficiency which was initially the main target to be improved in NOMA technique. Furthermore, frequency reuse at different UEs and cells potentially gives rise to interference in channel estimation, also known as pilot contamination [8]. These aforementioned problems can cause poor UE reception and degrade system performance.

In cellular uplink, the receiver performance typically depends on the quality and the estimation accuracy of CSI. Therefore, it is important to study the impact of CSI mismatch on the receiver reliability in NOMA systems. Although there exist a number of works on pilot decontamination, it is required to impose certain stringent conditions or costly mechanisms [9], [10]. Instead of focusing on improving CSI estimation by increasing pilot length, we aim to develop a robust receiver for NOMA systems against channel uncertainty. Given imperfect CSI, a plurality of robust receivers have been proposed in [11]–[13] to decode the data sent from the transmitter of interest while rejecting co-channel interference. In these works, the proposed receivers were designed based on minimum output energy (MOE) criterion, which minimizes the output power subject to bounded distortion in the recovered

1536-1276 © 2019 IEEE. Personal use is permitted, but republication/redistribution requires IEEE permission. See http://www.ieee.org/publications\_standards/publications/rights/index.html for more information.

transmitter-of-interest signal. These MOE-based receivers are able to handle moderate channel estimate errors. We aim to investigate improved robust receivers to ensure reliable data transmission in the presence of more significant CSI errors.

For NOMA systems, the performance of improved decoders together with SIC receiver have been analyzed under imperfect channel estimation [14], [15]. To better combat pilot contamination, we emphasize the benefit and the importance of exploiting additional error correction code characteristics to enhance performance [16], [17]. In the literature, the authors of [18] and [19] have proposed joint detection and decoding schemes, in which forward error correction (FEC) codes are applied as distinct UE signatures to construct the multi-user receiver under pilot contamination in massive multiple-input-multiple-output (MIMO) systems. Furthermore, for NOMA implementation, code word level interference cancellation are known to provide better performance than symbol level interference cancellation at the expense of higher overhead and complexity [2], [20].

In this paper, our emphasis is to overcome the reliance of NOMA systems on accurate CSI in achieving multi-user gains. We view this challenge of MUST implementation as an opportunity to exploit the intrinsic diversity of FEC code configurations. We propose a novel idea of NOMA receiver design with the integration of FEC codes to separate different pilot-interfering and data-multiplexing UEs during signal recovery. Utilizing each user signal's distinct FEC code as a unique signature, we reformulate an MOE-based minimum variance (MV) receiver as an unconstrained quadratic program by relaxing a strict distortionless response-preserving constraint. We subsequently integrate a set of FEC code permutations into our receiver to achieve better robustness against channel estimation errors (or channel uncertainty). Additionally, we propose enhancement methods of iterative detection and FEC code concatenation to further improve performance. Our code-anchored quadratic programming (CQP) receiver can contribute to the practical success of NOMA systems and is expected to ease error propagation in SIC process.

The remainder of the paper is organized as follows. In Section II, we develop the signal models for uplink NOMA system under channel uncertainty. Our proposed CQP receiver with integration of channel code is formulated in Section III as well as further performance enhancement by introducing iterative receiver and serial concatenation of FEC codes. Performance analysis of the proposed CQP receiver is derived in Section IV. In Section V, numerical results are provided along with the performance comparison with legacy receivers. Finally, concluding remarks are presented in Section VI.

*Notations:* Let bold capital and bold lowercase letters denote matrices and vectors, respectively. The transpose, Hermitian transpose, inverse, trace, and norm of a matrix are respectively presented in  $(\cdot)^T$ ,  $(\cdot)^H$ ,  $(\cdot)^{-1}$ ,  $\mathrm{tr}\{\cdot\}$ , and  $\|\cdot\|$ , respectively. A linear transformation which converts a matrix into a column vector is denoted as  $\mathrm{vec}(\cdot)$ .  $\mathbb{E}[\cdot]$  represents the statistical expectation over random variables. Notations  $\mathbb{R}^{m\times n}$  and  $\mathbb{C}^{m\times n}$  denote the set of  $m\times n$  matrices over real field and complex field, respectively.  $\mathrm{Re}\{\cdot\}$  and  $\mathrm{Im}\{\cdot\}$  denote the real

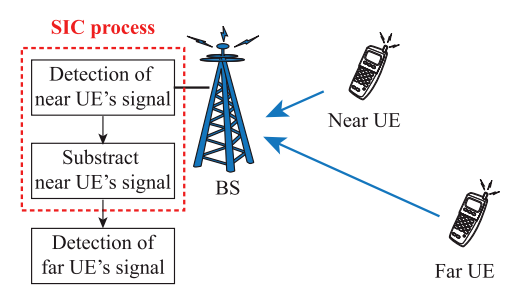


Fig. 1. Uplink NOMA transmission.

and imaginary parts of a complex value. An all-ones column vector of length n is denoted by  $\mathbf{1}_n$ . A standard basis vector is denoted by  $\mathbf{e}_n$  whose elements are all zero except for a 1 in its n-th position.  $\mathbf{I}_n$  is an identity matrix of size  $n \times n$ .  $\mathbf{A} \otimes \mathbf{B}$  denotes the Kronecker product of matrices  $\mathbf{A}$  and  $\mathbf{B}$ .  $\mathcal{CN}(\mu, \sigma^2)$  means a complex Gaussian random variable with mean  $\mu$  and variance  $\sigma^2$ .

# II. UPLINK NOMA SYSTEM UNDER CHANNEL UNCERTAINTY

#### A. Uplink Transmission

In this paper, a typical uplink single-cell scenario with NOMA technique is considered. A group of UEs  $\mathcal{K}=\{1,2,\cdots,K\}$  share the same uplink channels and transmit data to a base station (BS) simultaneously. As schematically shown in Fig. 1, a case of two UEs is given as an example. The BS is equipped with  $N_r$  received antennas and can support two or more UEs by superposition coding; while each UE unit is assumed to have  $N_t$  transmit antennas. In addition, we consider the case of  $N_r < KN_t$ , in which massive connectivity can be enabled by system overloading featured in NOMA scheme.

The conceptual block diagram for both the transmitter and receiver of uplink NOMA scheme is depicted in Fig. 2. At the transmitter side, the signal processing of NOMA system is the same as the one for orthogonal frequency-division multiple access (OFDMA). The information bit stream from each UE is firstly encoded by adding parity check bits for error correction, and the bit-level interleaver will spread out the bit stream. Without repeating or omitting any of the source data in the set, the UE-specific interleaving randomizes the bit sequence order so that the impact on any data stream is less concentrated when packets are lost, which further brings the benefit in terms of combating frequency selective fading and interference. The sequence of bits is then mapped to specific constellation points to generate the transmitted symbols. Thereafter, the data symbols of all UEs are transmitted over a frequency selectivechannel in the presence of additive white Gaussian noise (AWGN). The uplink channels from UEs to the serving BS are characterized by flat fading and can be denoted as H = $[\mathbf{H}_1, \mathbf{H}_2, \dots, \mathbf{H}_K] \in \mathbb{C}^{N_r \times KN_t}$ , where  $\mathbf{H}_k$  is the channel matrix associated with the k-th UE and can be written as

$$\mathbf{H}_{k} = \begin{bmatrix} h_{1,k,1} & h_{1,k,2} & \dots & h_{1,k,N_{t}} \\ h_{2,k,1} & x_{2,k,2} & \dots & h_{2,k,N_{t}} \\ \vdots & \vdots & \ddots & \vdots \\ h_{N_{r},k,1} & h_{N_{r},k,2} & \dots & h_{N_{r},k,N_{t}} \end{bmatrix} \in \mathbb{C}^{N_{r} \times N_{t}}, \quad (1)$$

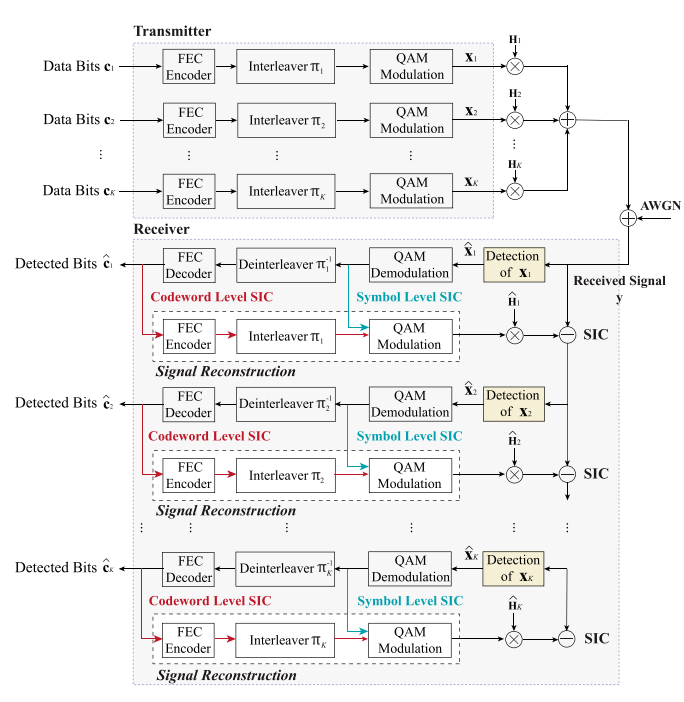


Fig. 2. Structure of signal processes in uplink NOMA scheme.

in which  $h_{m,k,n}$  denotes the gain coefficient from the n-th transmitted antenna of k-th UE to the m-th received antenna of BS. To be specific,  $h_{m,k,n} = g_{m,k,n} \sqrt{d_k}$  is composed of both large-scale attenuation factor  $\sqrt{d_k} \leq 1$  and small-scale fading coefficient  $g_{m,k,n} \sim \mathcal{CN}(0,1)$ .

As the UEs do have exclusive use of the frequency resource, the symbols from all UEs will be superimposed at the receiver. Therefore, the received signal vector at BS can be expressed as

$$\mathbf{y} = \tilde{\mathbf{H}}\tilde{\mathbf{x}} + \mathbf{n},\tag{2}$$

where  $\tilde{\mathbf{x}} = [\mathbf{x}_1, \mathbf{x}_2, \cdots, \mathbf{x}_K]^T \in \mathbb{C}^{KN_t \times 1}$  is the signal vector transmitted from all UEs of interest. Suppose antenna diversity technique is adopted at each transmitter, that is,  $\mathbf{x}_k = \frac{x_k}{\sqrt{N_t}} \cdot \mathbf{1}_{N_t}$ , where  $x_k$  is the data symbol of UE k with the normalization factor  $N_t$ . Also, data symbols in vector  $\tilde{\mathbf{x}}$  are modulated from source bit streams encoded by FEC codes, such as polar and capacity-approaching low-density parity-check (LDPC) codes.  $\mathbf{n} \in \mathbb{C}^{N_r \times 1}$  is a complex Gaussian noise vector distributed as  $\mathcal{CN}(\mathbf{0}, \sigma^2 \mathbf{I}_{N_r})$ , where  $\sigma^2$  is noise power. Notably, since NOMA is assumed to be on the basis of orthogonal frequency division multiplexing (OFDM) signaling with cyclic prefix (CP), the inter-symbol interference (ISI) and inter-carrier interference can be perfectly eliminated when the length of CP is sufficiently long to cover the multi-path delay spread.

# B. Channel Acquisition

In order to achieve accurate signal detection and decoding, most communication systems acquire channel state information (CSI) based on the known training pilots transmitted in regular time intervals. OFDM presents the advantages of simple and efficient implementation by using fast Fourier transform (FFT) and inverse fast Fourier transform (IFFT)

while inserting the cyclic prefix (CP) to remove inter-block interference. If the CP is at least equal to the channel delay spread in length, the N-FFT and IFFT would transform the frequency selective fading channel into parallel flat fading channels across N subcarriers. Then, the received signals at pilot subcarriers are used to perform channel estimation. Once the channel response of a dense set of subcarriers is obtained, channel responses overall N subcarriers can be interpolated.

However, training based channel estimates are typically corrupted by channel noise. In practice, the pilot signal of each UE probes only a limited number of subcarriers such that the channel interpolation might lead to further performance degradation. In the regime of very large number of antennas, another source of degradation is pilot contamination due to the aggressive frequency reuse in adjacent cells [8]. Especially in the NOMA systems accommodating a large number of mobile UEs, the effect of pilot contamination can be severe. Mathematically, if there are interfering UEs using the same set of training sequences synchronously, a linear channel estimator can output the estimated channel as well as its corresponding error variance [21], [22]. To characterize the impact of imperfect channel information, the estimated channel matrix of k-th UE available at BS is modeled as

$$\hat{\mathbf{H}}_k = \mathbf{H}_k + \Delta \mathbf{H}_k + \mathbf{N}_k,\tag{3}$$

where  $\Delta \mathbf{H}_k$  is the estimation error caused by the set of interfering UEs and  $\mathbf{N}_k$  is the error term associated with channel estimates [23]. In the following sections, we will investigate the impact of this imperfect channel estimation on interference cancellation before developing a receiver that is robust to such channel uncertainty.

## C. NOMA With SIC Receivers

Once the superimposed signal y is received at BS, a series of signal processing steps are employed to retrieve each UE's desired signal, as schematically shown in Fig. 2. In general, UE with stronger channel gain is decoded first to ensure that BS can detect this UE's message with higher accuracy while treating weaker users' signals as nuisance or noise. In an ideal SIC implementation, the BS generates a replica of the strong interfering signal that it has been successfully detected before subtracting it from the received signals so as to eliminate its effects on subsequent detection of other weaker UEs. However, due to channel noises and channel estimation errors, the strong UE's detection is prone to errors. Thus, error propagation in interference cancellation for weaker UEs is inevitable. In order to suppress the inter-user interference, the symbol level SIC (SSIC) receiver had been studied in [24] and [25]. From the perspective of SSIC receiver, the interfering symbols are detected and canceled without decoding, namely, the decision is made before error correction. To take the advantage of inherent FEC, the code word level SIC (CSIC) receiver further decodes the data bits rather than only data symbols in SSIC [15], [26]–[28]. Therefore, the error propagation caused by imperfect channel estimation can be somewhat mitigated at the expense of higher implementation complexity owing to FEC decoding.

To further enhance system performance, the design of a linear receiver, denoted as  $\mathbf{W}_k \in \mathbb{C}^{N_r \times N_t}$  for UE k, will be proposed to cooperate with aforementioned SSIC and CSIC schemes. Without loss of generality, we assume UEs  $\mathcal{K}$  are arranged in descending order of estimated channel gain, i.e.,  $\|\hat{\mathbf{H}}_1\|^2 \geq \|\hat{\mathbf{H}}_2\|^2 \geq \cdots \geq \|\hat{\mathbf{H}}_K\|^2$ . As the signals of UEs with stronger channel gain are detected, SIC can be performed to effectively cancel the inter-user interference. Hence, the signal at the input of the detector  $\mathbf{W}_k$  for UE k can be written as

$$\hat{\mathbf{y}}_k = \mathbf{y} - \sum_{k' < k}^K \hat{\mathbf{H}}_{k'} \hat{\mathbf{x}}_{k'}, \quad k = 1, 2, \dots, K.$$
 (4)

Since FEC decoding is not involved in SSIC, the estimated signal vector of UE k after SIC processing can be described by

$$\hat{\mathbf{x}}_k = \mathbf{W}_k^H \hat{\mathbf{y}}_k,\tag{5}$$

where (5) is used to denote signal detection at the symbol level, whereas the CSIC receiver further fed the estimated data symbol into an FEC decoder for error correction. Since FEC decoding is applied in the signal reconstruction of CSIC, the probability of successful recovery of signal will increase significantly compared with that in SSIC.

Compared with the traditional OMA technology, NOMA provides more access points for UEs to support massive connections. However, it also brings crucial inter-user interference problem. In addition, the mismatched receiver design based on the use of imperfect channel information will lead to the error propagation in SIC. It can be seen from (4) and (5) that the quality of signal detection can be improved by iteratively updating  $\hat{\mathbf{y}}_k$ , which motivates the proposal of advanced receiver design for multi-user detection (MUD) in the next section.

#### III. PROPOSED FEC CODE-ENHANCED SIC RECEIVER

In this section, our goal is to design a linear receiver  $\hat{\mathbf{W}} = [\mathbf{W}_1, \mathbf{W}_2, \cdots, \mathbf{W}_K] \in \mathbb{C}^{N_r \times KN_t}$  which is robust against imperfect channel knowledge at receiver. In such a receiver design, FEC code information is exploited as the distinct feature of UE's signature, which can help to retain the target UE's signal from that of interfering UEs while effectively suppressing inter-user interference despite of channel uncertainty and signal superposition in NOMA systems.

# A. MOE-Based MV Linear Receiver

In the NOMA case, the performance at receiver is highly dominated by the inter-user interference since the received signal is given by a superposition of signals sent from different UEs. Motivated by this fact, the key idea of our receiver is inspired by the well-established MOE approach adopted in MUD [29]. MOE receiver is one of the interference suppression criteria in code division multiple access (CDMA) that mitigates co-channel interference as much as possible while preserving a distortionless response to the UE of interest [30], [31].

Without loss of generality, let us assume the k-th UE is the UE of interest. Given the matrix  $\mathbf{W}_k$ , the output vector of information symbols of a linear receiver can be computed as (5) by using the vectorized model (4). For each entry of the symbol vector  $\hat{\mathbf{x}}_k$ , our main goal is to minimize output power at receiver and preserve a unity gain for this particular entry of  $\hat{\mathbf{x}}_k$  as well. A specific MV detector based on the MOE criterion had been proposed in [11]. The corresponding optimization problem is given by

$$\min_{\mathbf{W}_k} \operatorname{tr}\{\mathbf{W}_k^H \mathbf{R}_k \mathbf{W}_k\} \tag{6a}$$

s.t. 
$$\mathbf{W}_k^H \hat{\mathbf{H}}_k = \mathbf{I}_{N_t},$$
 (6b)

where  $\mathbf{R}_k = \mathbb{E}[\hat{\mathbf{y}}_k \hat{\mathbf{y}}_k^H] \in \mathbb{R}^{N_r \times N_r}$  is the covariance matrix of the vectorized received signal  $\hat{\mathbf{y}}_k$ . In practice, not all channel information and noise variance are available at the receiver, namely, the covariance matrix can not be computed directly. Alternatively, the true covariance matrix  $\mathbf{R}_k$  can be replaced by its sample estimate as

$$\hat{\mathbf{R}}_k = \frac{1}{T} \sum_{t=1}^{T} \hat{\mathbf{y}}_k(t) \hat{\mathbf{y}}_k^H(t), \tag{7}$$

where T is the available number of received signal blocks and  $\hat{\mathbf{y}}_k(t)$  is the t-th received signal block. To make the MV receiver given in [32] robust against finite sample effects and strengthen the condition number of  $\hat{\mathbf{R}}_k$ , a diagonal loading (DL) approach can be applied as in [33]. The closed-form expression for DL-based MV (DLMV) receiver is given as

$$\mathbf{W}_{k}^{(\text{DLMV})} = \tilde{\mathbf{R}}_{k}^{-1} \hat{\mathbf{H}}_{k} \frac{1}{\hat{\mathbf{H}}_{k}^{H} \tilde{\mathbf{R}}_{k}^{-1} \hat{\mathbf{H}}_{k}}, \tag{8}$$

where  $\tilde{\mathbf{R}}_k = (\hat{\mathbf{R}}_k + \delta \mathbf{I}_{N_r})$  is the DL-based covariance matrix and  $\delta$  is the DL factor.

# B. Quadratic-Programming Reformulation

Although the receiver (8) is able to reject co-channel interference under mild channel uncertainty, such an MV receiver is not easily amenable for further enhancement since it relies on the sufficiently accurate channel information  $\hat{\mathbf{H}}_k$ . When the channel uncertainty is substantial, the response-preserving constraint in (6b) may be error-prone and degrade the receiver's performance. It is important to emphasize that the complete cancellation of inter-user interference is a strongly desirable feature because otherwise, the imperfect SIC will cause error propagation in subsequent decoding of the signals of NOMA UEs. To remedy the noted shortcomings, the MV receiver is reformulated through a quadratic programming approach, and an artificial penalty is introduced to convert the original constrained problem into an unconstrained one.

Let the dummy parameter  $\tilde{\mathbf{w}}_k = \text{vec}(\mathbf{W}_k)$  be the vectorized receiver of matrix  $\mathbf{W}_k$ . Specifically, the vectorization of an  $N_r \times N_t$  matrix  $\mathbf{W}_k$  is the  $N_r N_t \times 1$  column vector obtained by stacking the columns of matrix  $\mathbf{W}_k$  on top of one another. Then, the cost function in (6a) can be reformulated in quadratic form as

$$\operatorname{tr}\{\mathbf{W}_{k}^{H}\tilde{\mathbf{R}}_{k}\mathbf{W}_{k}\} = \tilde{\mathbf{w}}_{k}^{H}\left(\mathbf{I}_{N_{t}} \otimes \tilde{\mathbf{R}}_{k}\right) \tilde{\mathbf{w}}_{k}.$$
 (9)

Follow the vectorization strategy, the constraint in (6b) can be reformulated in the similar manner as

$$\left(\mathbf{I}_{N_t} \otimes \hat{\mathbf{H}}_k^H\right) \tilde{\mathbf{w}}_k = \left[\mathbf{e}_1^T, \mathbf{e}_2^T, \cdots, \mathbf{e}_{N_t}^T\right]^T, \tag{10}$$

where the unit vectors  $\mathbf{e}_1, \mathbf{e}_2, \cdots, \mathbf{e}_{N_t}$  constitute the vectorization of identity matrix  $\mathbf{I}_{N_t}$ . For simplicity, we denote  $\mathbf{e} = \left[\mathbf{e}_1^T, \mathbf{e}_2^T, \cdots, \mathbf{e}_{N_t}^T\right]^T$ .

Since the imperfect channel information is taken into account, (6b) is reformulated as interference residue  $\|(\mathbf{I}_{N_t} \otimes \hat{\mathbf{H}}_k^H) \tilde{\mathbf{w}}_k - \mathbf{e}\|^2$ , which is used as a penalty term to enforce less stringent constraint on response preservation. The reformulation of (6) is formed by adding a penalty term to the cost function that consists of a penalty parameter multiplied by a measure of violation of the constraints, which can help to transform into an unconstrained quadratic programming formulation as

$$\min_{\tilde{\mathbf{w}}_k} \tilde{\mathbf{w}}_k^H \left( \mathbf{I}_{N_t} \otimes \tilde{\mathbf{R}}_k \right) \tilde{\mathbf{w}}_k + \gamma \| (\mathbf{I}_{N_t} \otimes \hat{\mathbf{H}}_k^H) \tilde{\mathbf{w}}_k - \mathbf{e} \|^2, \quad (11)$$

where  $\gamma$  is a regularization parameter. It is noted that the value of  $\gamma$  can be selected by trial and error in practice, which depends on the severity of interference and noise. Based on the similar vectorization strategy, the recovered data symbol of UE k in (5) can be rewritten as

$$\hat{x}_k = \tilde{\mathbf{w}}_k^H \cdot \text{vec}(\hat{\mathbf{y}}_k \otimes \mathbf{1}_{N_c}^T). \tag{12}$$

In order to obtain the desired message from the superimposed signal, additional signal constraints will be introduced to strengthen the performance of receiver design. In particular, the UE signatures presented by inherent FEC code information are exploited as distinct features. Therefore, a set of linear programming constraints will be introduced and incorporated into a unified receiver optimization process over the code word polytope.

#### C. Code Diversity Integration

In the following sections, we focus on signal recovery of one specific UE k so that the UE index k in the above formulations can be omitted without loss of generality. To strengthen the receiver robustness given imperfect channel estimates, a novel idea by exploiting FEC code diversity is advocated during signal recovery. Consider a linear code of length  $N_c$  and rate  $r = \frac{K_c}{N_c}$ , where  $K_c < N_c$  is the number of information bits in a code word. Let  $\mathcal{I}$  and  $\mathcal{J}$  be the sets of variable nodes and check nodes of the parity check matrix  $\mathbf{P}$ , respectively, i.e.,  $\mathcal{I} = \{1, \cdots, N_c\}$  and  $\mathcal{J} = \{1, \cdots, N_c - K_c\}$ .

To define a local code word, the neighbor set of a given check node  $j \in \mathcal{J}$  is denoted as  $\mathcal{N}_j$ . A parity check node can only be satisfied with one particular subset  $\mathcal{F} \subseteq \mathcal{N}_j$  that have even weight on its neighborhood variables. For each  $\mathcal{F}$  in the set  $\mathcal{S}_j \triangleq \{\mathcal{F} | \mathcal{F} \subseteq \mathcal{N}_j \text{ with } |\mathcal{F}| \text{ is even} \}$ , an auxiliary variable  $v_{j,\mathcal{F}} \in \{0,1\}$  is introduced as an indicator for local code word associated with  $\mathcal{F}$ . The global code word corresponds to the intersection of all the local codewords, which generally requires an explicit characterization of the constraints. Based on the method of linear programming relaxation [34], a more

manageable representation that is satisfied by every code word can be given by

$$\sum_{\mathcal{F}\in\mathcal{S}_j} v_{j,\mathcal{F}} = 1, \quad \forall j \in \mathcal{J}. \tag{13}$$

Furthermore, we use  $c_i \in \{0,1\}$ , where  $i \in \mathcal{I}$ , to denote each bit variable. Naturally,  $c_i$  must belong to the local code word associated with check node j, which leads to the following constraint:

$$\sum_{\mathcal{F} \in \mathcal{S}_{i}, i \in \mathcal{F}} v_{j,\mathcal{F}} = c_{i}, \quad \forall i \in \mathcal{I}, \ \forall j \in \mathcal{J}.$$
 (14)

Obviously, the code constraints (13) and (14) enforced for every parity check characterize a valid code word. To develop a unified receiver for signal transmissions in NOMA system, additional constraints that connect the recovered symbols in (12) to the bit variables  $\{c_i\}_{i\in\mathcal{I}}$  are required. In the following, we first outline the linear constraints for widely used QAM modulation. The joint detection method with a specific class of affine mapping between the binary data bits from the encoder and the modulated QAM symbols is then provided.

# D. Symbol Mapping Constraints

In order to integrate the code word constraints (13) and (14) into our linear programming framework, additional constraints are necessary to connect the detected symbols to the bit variable  $c_i$ . Generally, variables for bits and symbols in M-QAM can be linked by introducing indicator  $q_{d,m}$  [35], which is given by

$$\sum_{m=1}^{M} q_{d,m} = 1, \quad q_{d,m} \ge 0,$$

$$\forall d \in \mathcal{D} = \{1, 2, \dots, \frac{N_c}{\log_2 M}\}, \quad \forall m \in \mathcal{M} = \{1, 2, \dots, M\},$$
(15)

where d and m are the indexes of data symbols and signal constellation respectively. Furthermore,  $\{s_{d,m}\}_{d\in\mathcal{D},m\in\mathcal{M}}$  is introduced as signal constellation points in the M-ary QAM. The following linear constraints of d-th symbol for generic QAM were given in [36]

$$\operatorname{Re}\{\tilde{\mathbf{w}}^{H} \cdot \operatorname{vec}(\hat{\mathbf{y}}[d] \otimes \mathbf{1}_{N_{t}}^{T})\}$$

$$= \sum_{m=1}^{M} q_{d,m} \operatorname{Re}\{s_{d,m}\}, \quad \forall d \in \mathcal{D}, \qquad (16a)$$

$$\operatorname{Im}\{\tilde{\mathbf{w}}^{H} \cdot \operatorname{vec}(\hat{\mathbf{y}}[d] \otimes \mathbf{1}_{N_{t}}^{T})\}$$

$$= \sum_{m=1}^{M} q_{d,m} \operatorname{Im}\{s_{d,m}\}, \quad \forall d \in \mathcal{D}, \qquad (16b)$$

$$\sum_{m \in \mathcal{X}_{d,l}^{1}} q_{d,m} = c_{\log_{2} M \cdot (d-1) + l}, \quad \forall l = \{1, 2, \dots, \log_{2} M\}, \qquad (16c)$$

where the set  $\mathcal{X}_{d,l}^1 = \{m \in \mathcal{M} | (l\text{-th bit of } s_{d,m}) = 1\}$  contains the symbol indices whose bit representation has a "1" in the l-th position.

In (16), however, general high-order QAM constellations with practical mapping, e.g., Gray-code, is not amenable to affine relationships as the cases for BPSK and QPSK modulations between bits and symbols. Without loss of generality, the bit-to-symbol mapping for QPSK adopted in this work can be formulated as

$$\operatorname{Re}\{\tilde{\mathbf{w}}^{H} \cdot \operatorname{vec}(\hat{\mathbf{y}}[d] \otimes \mathbf{1}_{N_{t}}^{T})\} = (1 - 2 \cdot c_{2d-1}) / \sqrt{2}, \quad \forall d \in \mathcal{D},$$

$$(17a)$$

$$\operatorname{Im}\{\tilde{\mathbf{w}}^{H} \cdot \operatorname{vec}(\hat{\mathbf{y}}[d] \otimes \mathbf{1}_{N_{t}}^{T})\} = (1 - 2 \cdot c_{2d}) / \sqrt{2}, \quad \forall d \in \mathcal{D}.$$

$$(17b)$$

Together with (17), the integration of code constraints (13) and (14) into the quadratic program (11) can be used to exploit the distinct features of code configurations.

#### E. Code-Anchored Quadratic Programming (CQP) Receiver

To strengthen the SIC receiver robustness given imperfect channel estimates, a unified receiver is advocated by the joint design of detection and decoding algorithm. The optimization problem relies on a single unified objective function with integration of a set of linear constraints that are generated from parity checks [34].

The difficulty of solving the integer programming problem in (11) arises from the integer constraints  $v_{j,\mathcal{F}} \in \{0,1\}$  and  $c_i \in \{0,1\}$ , which will lead to high computational complexity. Before we finalize our joint quadratic programming receiver integrated with code constraints, the continuous relaxation is adopted by relaxing the binary indicators  $v_{j,\mathcal{F}}$  and  $c_i$  to  $0 \leq v_{j,\mathcal{F}} \leq 1$  and  $0 \leq c_i \leq 1$  respectively. While the detected symbols  $\hat{x} = \tilde{\mathbf{w}}^H \cdot \text{vec}(\hat{\mathbf{y}} \otimes \mathbf{1}_{N_t}^T)$  can not be quantized, they can be further processed by soft decoding for better performance. Therefore, a linear programming relaxation of the original problem is achieved as

$$\min_{\tilde{\mathbf{w}}, \boldsymbol{v}, \mathbf{c}} \tilde{\mathbf{w}}^{H} \left( \mathbf{I}_{N_{t}} \otimes \tilde{\mathbf{R}} \right) \tilde{\mathbf{w}} + \gamma \| (\mathbf{I}_{N_{t}} \otimes \hat{\mathbf{H}}^{H}) \tilde{\mathbf{w}} - \mathbf{e} \|^{2} \quad (18a)$$
s.t.  $\operatorname{Re} \{ \tilde{\mathbf{w}}^{H} \cdot \operatorname{vec}(\hat{\mathbf{y}}[d] \otimes \mathbf{1}_{N_{t}}^{T}) \} = \frac{1 - 2 \cdot c_{2d-1}}{\sqrt{2}}, \quad \forall d \in \mathcal{D},$ 

$$\operatorname{Im} \{ \tilde{\mathbf{w}}^{H} \cdot \operatorname{vec}(\hat{\mathbf{y}}[d] \otimes \mathbf{1}_{N_{t}}^{T}) \} = \frac{1 - 2 \cdot c_{2d}}{\sqrt{2}}, \quad \forall d \in \mathcal{D},$$

$$\sum_{\mathcal{F} \in \mathcal{S}_j} v_{j,\mathcal{F}} = 1, \quad \forall j \in \mathcal{J}, \tag{18d}$$

$$\sum_{\mathcal{F} \in \mathcal{S}_j} v_{j,\mathcal{F}} = c_i, \quad \forall i \in \mathcal{I}, \ \forall j \in \mathcal{J},$$
(18e)

$$0 \le v_{j,\mathcal{F}} \le 1, \quad \forall j \in \mathcal{J}, \ \forall \mathcal{F} \in \mathcal{S}_j,$$
 (18f)

$$0 \le c_i \le 1, \quad \forall i \in \mathcal{I}, \tag{18g}$$

where  $\tilde{\mathbf{w}}$ ,  $\mathbf{v} \triangleq \{v_{j,\mathcal{F}} | \forall j \in \mathcal{J}, \forall \mathcal{F} \in \mathcal{S}_j\}$ , and  $\mathbf{c} \triangleq [c_1, c_2, \cdots, c_{N_c}]^T$  are the de-facto optimization arguments. It can be seen that our strategy aims to formulate a relaxed polytope that contains all the codewords, but has a more manageable representation. More specifically, each check node in linear programming terminology defines the set of convex combinations of local codewords. Our global relaxation

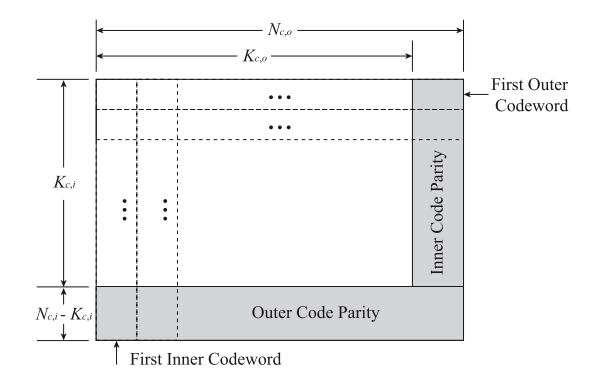


Fig. 3. Block diagram of concatenated code.

polytope will be the intersection of all of these local codes. To this end, off-the-shelf polynomial-time algorithms, such as interior-point methods, can be applied to solve this quadratic programming problem [37].

In this work, MUD problem is tackled by presenting a novel idea of adopting the FEC code diversity as unique signatures. Specifically in pilot contamination scenario, different FEC codes can be allocated to pilot-interfering UEs for the purpose of distinguishing target UE. In practice, however, the number of mobile UEs may far exceed the channel codes specified in the system standard. In such a case, different code word permutations can be applied by utilizing interleaving and transmit diversity, which reorders the sequence of code bits transmitted along different channels. Defining  $\Pi_k$  as the permutation matrix for UE k, the code word c will be interleaved by  $\Pi_k$  before modulation. Thus, bit variables  $c_i$ in bit-to-symbol mapping constraints (18) should be replaced by the permuted code word  $\tilde{\mathbf{c}}_k = \mathbf{\Pi}_k \mathbf{c}$  while those in code constraints remain unchanged. Thereby, the detrimental effects of pilot contamination in NOMA system is expected to be eliminated by adopting the proposed CQP receiver. Given bounded channel estimate errors, simulation results will show that our CQP receiver can effectively alleviate the impact of error propagation in SIC.

F. Performance Enhancement Through Iterative Receiver and Serial Concatenation of FEC Codes

While the spectral efficiency of NOMA is superior compared to OMA, the fact that the cluster-based UE coexistence causes performance degradation to the UEs with worse channel conditions. As iterative SIC is performed within each NOMA cluster, error propagation will be a crushing blow for MUD. In order to further improve the reliability of far UEs, our CQP receiver anchored with a single FEC code will be extended to serial concatenation of outer and inner codes.

For the purposes of these benchmarks, the encoding operation starts by hierarchically dividing the source information bits into several chunks each of small size, and some redundancy is added via an outer code. Then each data chunk is independently encoded into codewords via a separate inner code. As schematically shown in Fig. 3, the result is the transmitted code word where two FEC codes denoted by outer and inner codes are block-concatenated in the row and column directions, respectively. The outer code is a  $(N_{c,o}, K_{c,o})$  code

(18c)

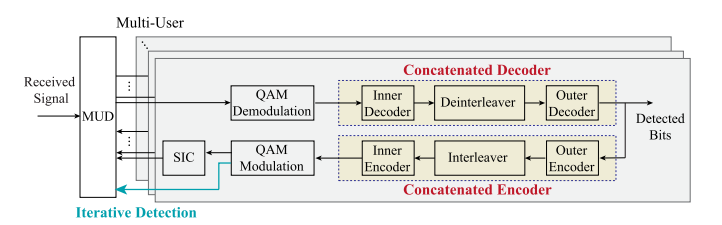


Fig. 4. Receiver with iterative detection and serial concatenated FEC codes.

whereas the inner code is a  $(N_{c,i}, K_{c,i})$  code. More specifically, the concatenation is also illustrated in Fig. 4, which means performing both encoding and decoding in two layers.

In this paper, a Reed-Solomon (RS) code serially concatenated to an LDPC code is considered. As the first decoding layer, the author in [38] have demonstrated that LDPC codes can achieve near capacity performance by soft-decoding algorithms of moderate complexity. LDPC code is identified by a sparse parity check matrix that is amenable to be characterized as linear signal constraints in our integrated receiver algorithm. The outputs of inner decoder are then fed to RS decoder, which retries decoding on the codewords that failed in the first place. Being responsible for further enhancement, the outer decoder as rough code should work well also in the presence of a large number of errors. Since RS code is strong to both burst and random errors [39], it is being widely used in the applications of communication and therefore chosen as outer code in this work. It is noted that the concatenated code construction can preserve the linearity of CQP receiver that is built upon. This is because both inner LDPC and outer RS codes have a linear encoding structure. As an extra level of interleaving, an interleaver is usually added between these two codes to spread error bursts across a wider

In uplink NOMA systems, SIC is acting in a serial manner majorly based on the channel gains of UEs. For near UEs, interference from far UEs which is treated as noise can degrade the decoding performance; while the performance of far UEs highly relies on the accuracy of decoding and canceling high power signals. Therefore, iterative signal processing is further carried out in order to detect and cancel inter-user interference specially passing iterative detection algorithm. As illustrated in Fig. 4, the detected signals of all UEs are fed back to multi-user detector (MUD) in addition to SIC for iterative detection. Employing multiple iterations of signal detection which is based on exploiting priori estimates obtained from the previous iteration can improve the detection and interference cancellation performances. The process continues in this fashion until either the decoder generates valid codewords for the entire UEs or enough attempts have been made.

With the iterative receiver and serial concatenation of FEC codes, the low error rate regime is expected to be achieved through the decay of error rate can be traded off with the computational complexity of signal decoding and detection. Also, it is noted that downlink NOMA brings more complexity because of the utilization of iterative detection procedures at multiple receive nodes, when compared to the central receiver, as applicable in uplink NOMA systems.

# IV. PERFORMANCE EVALUATION AND COMPLEXITY ANALYSIS

## A. Performance Upper Bound

In order to provide insightful results about the quality of proposed CQP receiver, it is crucial to study the error rate performance of each individual NOMA UE while considering channel error-induced imperfect SIC. Consequently, the received signal-to-interference-plus-noise ratio (SINR) and average bit error rate (BER) analysis are presented in this section.

Accurate BER analysis of NOMA systems is intractable since the exact calculation requires prohibitively high computational complexity due to the SIC process. However, pairwise error probability (PEP) can be analyzed based on the Bhattacharyya parameter in conjunction with the union bound and weight enumeration [40]. It is worth mentioned that PEP gives a valuable indicator for the BER analysis since it is viewed as an upper bound for BER performance. Emphasizing on this, we formulate a performance upper bound of coded BER for the proposed receiver by considering the error event with the minimum Hamming distance in the union bound, which is given by [41]

$$P_b^c = \frac{\bar{b}}{K_c} \le \frac{1}{K_c} \sum_{i=1}^{N_c} \bar{\varepsilon}_i P_p,$$
 (19)

where  $\bar{b}$  and  $K_c$  are the expected number of erroneous information bits and the number of information bits mentioned in Section III-C, respectively.  $\bar{\varepsilon}_i$  is the weight enumerator that can be calculated as  $\bar{\varepsilon}_i = \sum\limits_{j=1}^{K_c} \varepsilon_{i,j}$ , where  $\varepsilon_{i,j}$  is the number of codewords with weight i that corresponds to information sequence of weight j. The code word PEP is denoted as  $P_p$ .

1) PEP Analysis of the Nearest UE: Prior to the PEP calculation, a brief overview of SINR expression which explicitly captures the effects of pilot contamination and interference cancellation is presented. Recall that the first UE in set  $\mathcal{K}$  is assumed to be the nearest UE with the strongest channel gain. Given the received signal vector in (2) with normalized transmit power  $\mathbb{E}[\|\mathbf{x}_k\|^2] = 1$  for all k, the received SINR of the nearest UE adopting receiver  $\mathbf{W}_1$  can be represented as

$$\Gamma_{1}(\mathbf{W}_{1}) = \frac{\|\mathbf{W}_{1}^{H}\mathbf{H}_{1}\|^{2}}{\sum_{k'=2}^{K} \|\mathbf{W}_{1}^{H}\mathbf{H}_{k'}\|^{2} + \underbrace{\sigma^{2}\|\mathbf{W}_{1}^{H}\|^{2}}_{\text{Noise power}}}.$$
 (20)

However, once the total received power of interferers contributing to pilot contamination is comparable to that of the desired UE, the SINR with a pilot corrupted estimation has higher probability that it is less than (20) of perfect estimation. As our proposed CQP receiver can improve MV receivers by incorporating the knowledge of FEC code, the performance of basic MV receiver is used as a baseline. Similar to DLMV receiver presented in (8), the MV receiver without DL factor is given by  $\mathbf{W}_1^{(MV)} = \hat{\mathbf{R}}_1^{-1}\hat{\mathbf{H}}_1(\hat{\mathbf{H}}_1^H\hat{\mathbf{R}}_1^{-1}\hat{\mathbf{H}}_1)^{-1}$ . It can be observed that MV receiver is a scaled minimum-meansquared-error (MMSE) receiver [42], which is presented as

 $\mathbf{W}_1^{(MMSE)} = \hat{\mathbf{R}}_1^{-1}\hat{\mathbf{H}}_1.$  By neglecting the noise effect, we have  $\Gamma_1(\mathbf{W}_1^{(MV)}) = \Gamma_1(\mathbf{W}_1^{(MMSE)}).$  The deterministic expression of SINR with an MMSE receiver is analyzed in [23] under pilot contamination as

$$\tilde{\Gamma}_{1}(\mathbf{W}_{1}^{(\text{MMSE})}) = \frac{\|(\mathbf{W}_{1}^{(\text{MMSE})})^{H}\mathbf{H}_{1}\|^{2}}{I_{1}^{(\text{P})} + \sum_{k'=2}^{K} \|(\mathbf{W}_{1}^{(\text{MMSE})})^{H}\mathbf{H}_{k'}\|^{2} + \sigma^{2}\|(\mathbf{W}_{1}^{(\text{MMSE})})^{H}\|^{2}}$$
(21)

where pilot interference  $I_1^{(P)} = \|(\mathbf{W}_1^{(\text{MMSE})})^H \Delta \mathbf{H}_1\|^2$  is introduced to capture the effect of imperfect channel estimation, which contributes negatively to the SINR in addition to interference averaging.

According to [43], the average symbol error probability (SEP) for M-QAM is given as

$$P_{s,1} = 1 - \left[1 - 2\left(1 - \frac{1}{\sqrt{M}}\right)Q\left(\sqrt{\frac{3\tilde{\Gamma}_1}{M-1}}\right)\right]^2,$$
 (22)

where  $Q(\cdot)$  is the Q-function. Assuming the symbol energy is equally divided among all bits and the Gray mapping is used, the uncoded BER performance is given by [44] and obtained as

$$P_{b,1}^u = P_{s,1}/\log_2 M. (23)$$

As every bit is treated equally, the equivalent channel model introduced for a bit-interleaved coded modulation (BICM) system can be adopted. The channel constituted by all the entities in Fig. 2 from the interleaver at the transmitter up to the deinterleaver at the receiver can be viewed as a memoryless binary symmetric channel (BSC) with a certain bit-flip probability  $P_{b,1}^u$ . For the BSC, a Bhattacharyya parameter associated with a channel is defined as  $\beta = 2\sqrt{P_{b,1}^u(1-P_{b,1}^u)}$ . By averaging over all possible codebooks, we invoke the Bhattacharyya upper bound [41] on the PEP to obtain

$$P_{p,1}(i) \le \beta^i, \tag{24}$$

where i is the Hamming distance between two codewords. To this end, the coded BER of nearest UE can be obtained by substituting (24) into (19), which is formulated as

$$P_{b,1}^c \le \frac{1}{K_c} \sum_{i=1}^{N_c} \sum_{j=1}^{K_c} \varepsilon_{i,j} \beta^i.$$
 (25)

2) PEP Analysis of Far UEs: For the k-th UE, the signals with higher power have been recovered to perform SIC before detecting its own signal. It is clear from (4) and (5) that the impact of mismatch signal reconstruction on SIC is a function of the iteration number and it is conditioned on the accuracy of the most recent detection of interferers' symbols. Therefore, the effective SINR of the k-th UE is represented as

$$\tilde{\Gamma}_{k}(\mathbf{W}_{k}^{(\text{MMSE})}) = \frac{\|(\mathbf{W}_{k}^{(\text{MMSE})})^{H}\mathbf{H}_{k}\|^{2}}{I_{k}^{(\text{P})} + \sum_{k'>k}^{K} \|(\mathbf{W}_{k}^{(\text{MMSE})})^{H}\mathbf{H}_{k'}\|^{2} + I_{k}^{(\text{R})} + \sigma^{2} \|(\mathbf{W}_{k}^{(\text{MMSE})})^{H}\|^{2}},$$
(26)

where the residual interference  $I_k^{(\mathrm{R})} = \sum_{k'' < k}^K P_{s,k''}$ 

 $\|(\mathbf{W}_k^{(\mathrm{MMSE})})^H \mathbf{H}_{k''}\|^2$  is the error statistic at the k-th iteration to the desired symbol.  $P_{s,k''}$  is the SEP of UEs with stronger channel condition, which can be calculated as shown in (22).

Based on (26), the PEP and coded BER of the k-th UE can be obtained as the similar way described in (24) and (25). As a final note, we currently provide a brief overview of performance upper bound based on MV receiver and Bhattacharyya parameter. A further derivation of tighter bound for those integrated formulations in our CQP receiver can be approximated in some closed-forms, which is left as the future work.

# B. CQP Complexity Analysis

In general, the cost of solving a quadratic programming problem via interior-point method is  $\mathcal{O}(N^3)$ , where N is the length of variable vector [45]. In (18), the proposed CQP receiver introduces more auxiliary variables and equality constraints to exploit FEC code diversity. For an  $(N_c, K_c)$ LDPC code with row weight  $\omega$  is assumed, the bit variable vector  $\mathbf{c} \in \mathbb{C}^{N_c \times 1}$  and the length of set indicator vector v is  $(N_c - K_c) \times 2^{\omega - 1}$ . Given  $\tilde{\mathbf{w}} \in \mathbb{C}^{N_r N_t \times 1}$ , there are  $N_r N_t + N_c + (N_c - K_c) \times 2^{\omega - 1}$  variables in total within the joint quadratic programming receiver. Furthermore, SIC receiver requires demodulation and decoding for other sets of UEs in addition to those for its own UE, in which iterative interference cancellation will increase time complexity with a linear scale K. The feasibility of NOMA implementation will highly depend on the evolution of device processing capabilities. This is a cumbersome task provided the limited processing capability of UEs in downlink transmission; whereas in uplink, it is relatively more convenient to implement MUD and interference cancellation by a centralized entity. Furthermore, limiting the number of multiplexed UEs per subcarrier can reduce SIC complexity at receiver. The other fact that increased complexity arose from code size as well as it's code weight structure, however, can be reduced thanks to LDPC code with sparse nature of parity check matrix.

#### V. NUMERICAL RESULTS

In this section, numerical results of proposed CQP receiver for uplink NOMA transmission are evaluated in term of BER. Without loss of generality, let K=2 in NOMA system. Throughout the simulation section, quasi-static Rayleigh fading channels are assumed. The large-scale channel gain between near UE and BS, denoted as  $d_1$  in (1), is normalized as 1; while that of far UE,  $d_2$ , is left as a control variable in simulations. A pilot-based channel estimation with 128 subcarriers and  $N_p$  pilots are considered. Channel coefficients in pilot subcarriers are estimated by using linear MMSE (LMMSE) algorithm and channel interpolation is performed by linear interpolation.

At the UE transmitter, the binary information sequence is encoded with the code rate of r and configured as  $N_c=256$ . Owing to the near-capacity performance, we focus on the

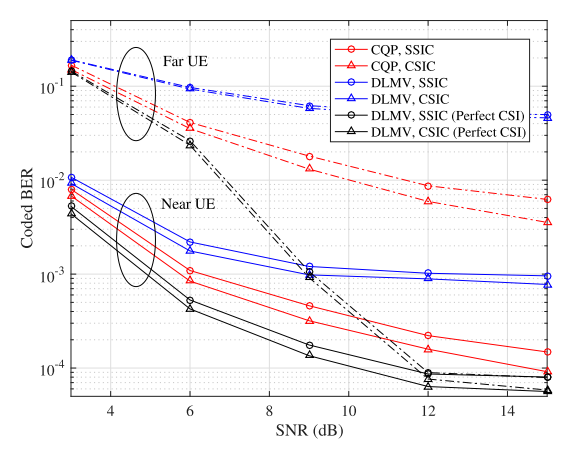


Fig. 5. Demonstration of code-anchored receiver benefits: BER versus SNR with LDPC code of r=3/4 under  $N_r=4$ ,  $N_t=1$ ,  $N_p=32$ , SIR = 10 dB, and channel power gains  $[d_1,d_2]=[1,0.3]$ .

practical and popular LDPC codes. A set of linear constraints (18b)-(18g) in unified receiver optimization process are generated from LDPC parity checks. Moreover, each UE's modulation scheme is the standard QPSK with Gray mapping. At the BS, off-the-shelf CVX solver [46] is applied to solve the optimization problem in (18). The regularization parameter  $\gamma=75$ . By using log-likelihood ratios (LLR) as messages between symbol and parity check nodes, efficient implementations of the sum-product algorithm (SPA) are adopted for decoding LDPC codes [47].

To reveal the merits of FEC code anchoring, the conventional DLMV receiver without code constraints, as shown in (8), is considered under both perfect and imperfect CSI as legacy baselines. At this moment, the numerical results do not compare with the theoretical upper bound provided in Section IV since the current bound obtained by using plain MV receiver appears to be rather loose. However, the performance of DLMV receiver can reach a better approximation due to the performance improvement through DL approach.

#### A. Benefits of Code Anchoring

To verify the gain promised by using FEC code configurations, the performance realized by different receivers joint with SSIC and CSIC are evaluated for comparisons. We consider 2 UEs in the uplink network with  $[d_1,d_2]=[1,0.3]$  to the BS, which characterizes the requirement of channel gain disparity in NOMA systems. The BS is equipped with 4 antennas while each UE is equipped with a single antenna. In channel estimation, the number of pilots  $N_p=32$  is used with signal-to-interference ratio (SIR) of pilot equals 10 dB. An LDPC code of rate r=3/4 is adopted.

In Fig. 5, we demonstrate the advantages of code-anchoring by illustrating the coded BER of DLMV and the proposed CQP receivers versus signal-to-noise ratio (SNR). It is noted that SNR is defined as the ratio of received signal intensity of superimposed signal to noise. Under the same CSI knowledge at receiver, the curves confirm the significant gains achievable by the proposed CQP receiver. Even though small  $d_2$  is chosen, the performance of far UE provided by CQP receiver surpasses the legacy baseline since DLMV receiver does not exploit FEC

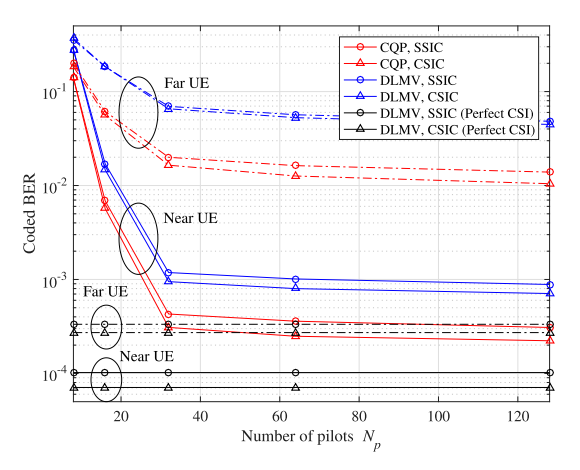


Fig. 6. BER versus number of pilots  $N_p$  with LDPC code of r=3/4 under  $N_r=4$ ,  $N_t=1$ , SNR = 10 dB, SIR = 10 dB, and channel power gains  $[d_1,d_2]=[1,0.3]$ .

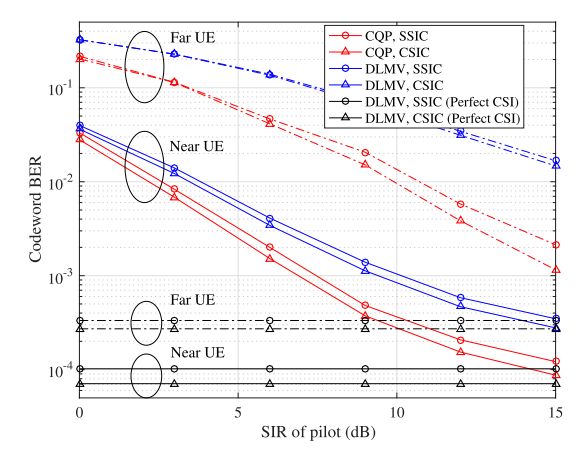


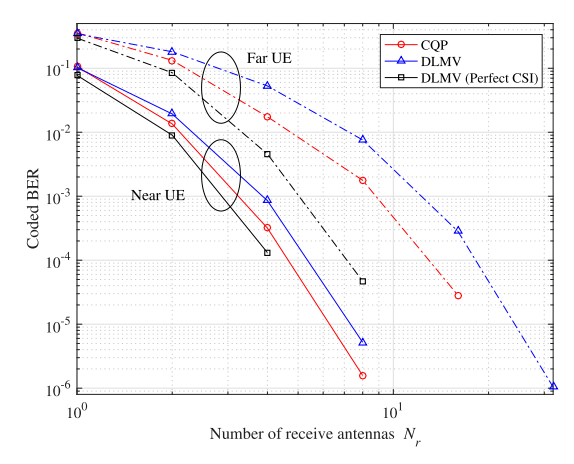
Fig. 7. BER versus SIR of pilot with LDPC code of r=3/4 under  $N_r=4$ ,  $N_t=1$ ,  $N_p=32$ , SNR = 10 dB, and channel power gains  $[d_1,d_2]=[1,0.3]$ .

code information. Furthermore, the required SNR of SSIC for achieving the same BER is higher than that of CSIC, which further validates that channel coding helps tolerate faults introduced by imperfect CSI. However, the coded BERs decrease with a sign of error floor due to unknown inter-user interference from farther UEs.

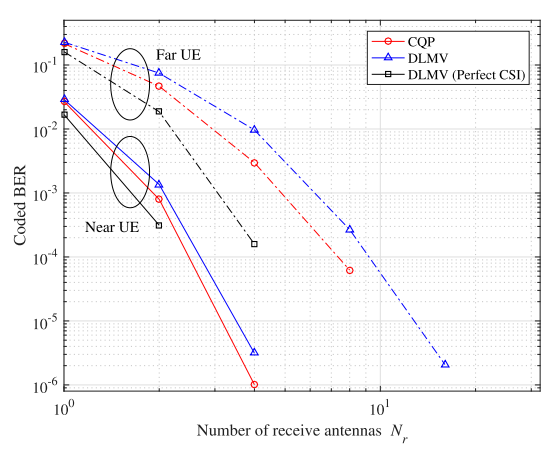
#### B. Impacts of Channel Estimation Errors

As interference cancellation in NOMA systems relies on channel knowledge at the destination receiver, the experiments are designed to evaluate the impact of channel estimation errors by illustrating the BER performance under channel uncertainty and pilot interference. To clearly demonstrate the mismatched CSI effects, the noise level is fixed as  $SNR = 10 \ dB$ .

Fig. 6 shows the BER performance under varying numbers of pilots  $N_p$ . As the increase of  $N_p$ , lower error rate can be achieved due to a more accurate channel estimate. It can also be observed that our CQP receiver is less sensitive to channel uncertainty, which is beneficial to deal with pilot shortage in NOMA systems. Moreover, we consider that the UE channel coefficient  $\mathbf{H}_k$  deviates from the channel estimate  $\hat{\mathbf{H}}_k$  with a specific set of SIR values. As shown in Fig. 7,



#### (a) Number of transmit antennas $N_t = 1$



(b) Number of transmit antennas  $N_t = 2$ 

Fig. 8. BER versus numbers of receive antennas  $N_r$  and transmit antennas  $N_t$  with LDPC code of r=3/4 under  $N_p=32$ , SNR = 10 dB, SIR = 10 dB, and channel power gains  $[d_1,d_2]=[1,0.3]$ .

the BER performance can be drastically improved for all the considered receivers when the SIR of pilot sequence increases. In contrast to DLMV receiver, which is clearly interference-limited, the proposed receiver can conquer the limit imposed by pilot interference to a great extent. Again, the performance gain obtained by joint receivers and CSIC can be observed from Fig. 7, which is the major combination selected in the following code word-level evaluations.

# C. Effect of Number of Antennas

In Fig. 8(a), we focus on exploiting multiple antennas technique in NOMA networks. A characterization of multiple antenna capacity is clarified and the effects of system dimensions are utilized for performance enhancement. By increasing the size of receive antenna array at given SNR and SIR, the curves show no sign of error floor but possess constant BER decrease. Based on the usage of multiple antennas with spatial diversity, we are able to average out the thermal noise at receiver [48]. Similarly, the space diversity is also found at transmitters to increase the transmission reliability, as illustrated in Fig. 8(b) with  $N_t=2$ . The above observations reaffirm the theoretical principle that large antenna array can

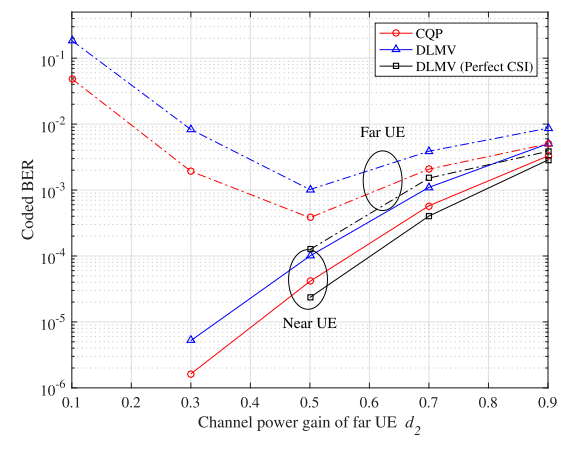


Fig. 9. BER versus channel power gains of far UE  $d_2$  with LDPC code of r=3/4 under  $N_p=32,\ N_r=8,\ N_t=1,\ {\rm SNR}=10$  dB, and  ${\rm SIR}=10$  dB.

improve system performance in terms of data rate and link reliability.

#### D. Impact of Channel Gain Disparity

In this section, the conventional near-far UE pairing concept in NOMA system is addressed. A far UE with varying channel gain  $d_2$  is multiplexed on a channel occupied by a near UE with normalized channel gain  $d_1 = 1$ . Since BS treats the signal of far UE as interference when detecting near UE's signal, the performance difference shown in Fig. 9 is observed not as a function of SIR but rather as depending on how disparate two UEs channels are. As opposed to BER increases with  $d_2$  at near UE, the error rate of far UE is improved due to stronger signal strength against noise. However, the performance of far UE decreases once again at an even higher level of  $d_2$ due to the degradation of interference cancellation accuracy, thus getting error propagation. From UEs' fairness standpoint, choosing a far UE with competing channel gain can guarantee a certain grade of fairness, but at the price of sacrificing the overall system performance. Therefore, their performance could be substantially compromised without proper design. Unlike conventional techniques, our CQP receiver strengthen the signal detection by using FEC code diversity, which provides more flexibility by allowing tradeoffs between UE fairness and overall system performance.

#### E. BER Comparisons with Different Code Configurations

Generally, FEC codes can provide strong protections against bit errors particularly in the cases of low code rates. In this test, we compare different combinations of code permutations by showing the coded BER versus given system parameters. In Fig. 10, the CQP receiver with an LDPC code of rates r=3/4 and r=1/2 are compared. At the expense of extra redundancy, it can be clearly seen that the receivers with r=1/2 code have more robust performance than that provided by receivers with r=3/4 code. Moreover, the proposed CQP receiver with iterative detection, which is termed as CQP-I, is evaluated. As mentioned in Section III-F, signal detection and SIC process can be enhanced by exploiting a priori estimate obtained from the previous iteration.

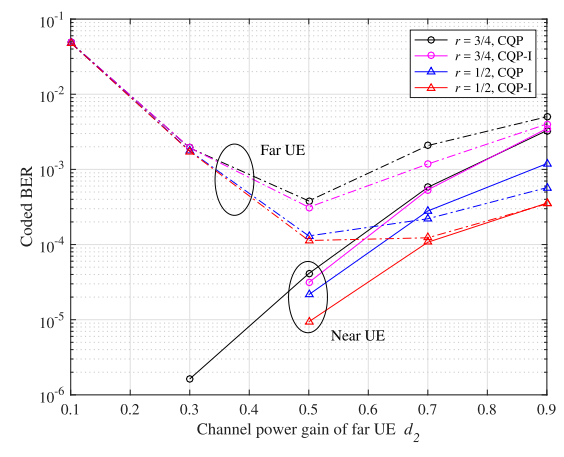


Fig. 10. BER versus channel power gains of far UE  $d_2$  with LDPC code of  $r=\{3/4,1/2\}$  under  $N_p=32,~N_r=8,~N_t=1,~{\rm SNR}=10~{\rm dB},$  and SIR = 10 dB.

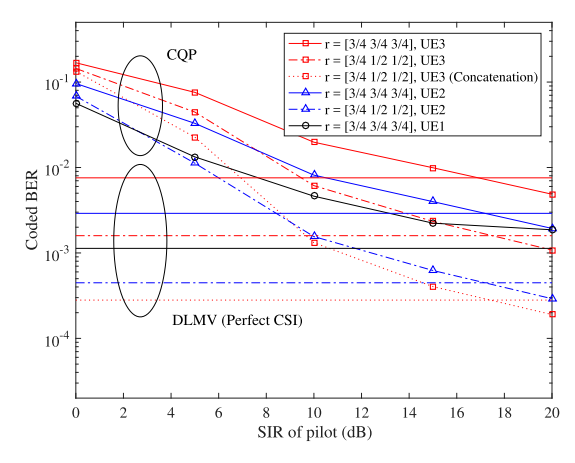
From the simulation results, it is observed that CQP-I can provide further performance enhancement, and the performance of these 2 UEs will converge to a specific value with almost the same channel gains.

Furthermore, the higher flexibility in NOMA implementation realized by our proposed receiver is demonstrated by considering the number of UEs K=3 under a given set of SIR values. A UE set with channel power gains  $[d_1,d_2,d_3]=[1,0.75,0.5]$  and  $[d_1,d_2,d_3]=[1,0.5,0.3]$  are evaluated and compared in Fig. 11(a) and Fig. 11(b), respectively. The CQP receiver with LDPC code of rate r=3/4 adopted by all UEs is first evaluated as a baseline. To face poor performance of far UEs, the code rates of UE 2 and 3 are replaced with r=1/2. As a final resort, the performance of the farthest UE, i.e., UE 3, is further enhanced by concatenating the original LDPC code with an outer RS (255,223) code.

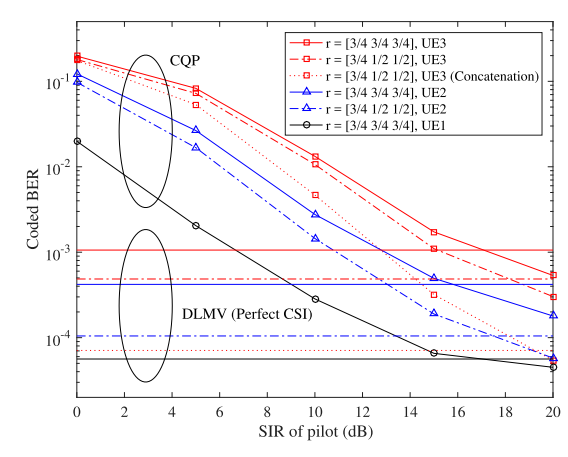
The results in Fig. 11 demonstrate that lower code rates and concatenated codes are helpful in reducing the error probability for channel coding, hence strengthen the robustness of proposed CQP receiver. By implementing lower code rate and FEC concatenation, the performance of far UEs can be improved while retaining good performance of near UE. When SIR of pilot sequence is sufficiently high, the interfering signals can be fully resolvable at previous SIC iterations. In this case, our proposed CQP receiver can achieve or even outperform the DLMV receiver designed based on perfect CSI. It is because our method is not only robust against pilot interference but also noise. Comparing the results of Figs. 11(a) and 11(b), to achieve a required BER, the proposed CQP receiver provides more flexible tradeoff between fairness and system performance, which conquers the limit imposed by the requirement of channel disparity in NOMA clustering to a great extent.

# F. Performance Analysis of Downlink NOMA Transmissions with CQP Receiver

As the final note, our proposed CQP receiver can also be used to lower error rate in downlink transmissions. For downlink NOMA systems, near UEs can decode and cancel all high power signals of paired UEs through SIC process;



(a) Channel power gain  $[d_1, d_2, d_3] = [1, 0.75, 0.5]$ 



(b) Channel power gain  $[d_1, d_2, d_3] = [1, 0.5, 0.3]$ 

Fig. 11. BER versus SIR under  $N_p = 32$ ,  $N_r = 8$ ,  $N_t = 1$ , SNR = 10 dB.

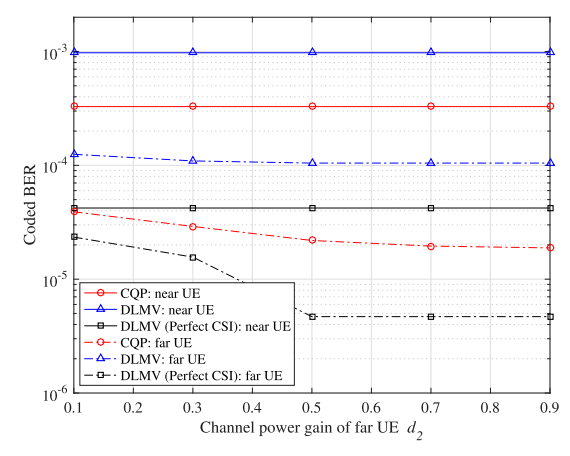


Fig. 12. Downlink BER versus channel power gains of far UE  $d_2$  with LDPC code of r=3/4 under  $N_p=32$ ,  $N_r=1$ ,  $N_t=8$ , SNR = 10 dB, SIR = 10 dB, and  $[\alpha_1,\alpha_2]=[\frac{1}{3},\frac{2}{3}]$ .

while far UEs recover their signals by treating other low power interfering signals as noise. Based on NOMA principle, BS allocates more power to the UEs with weaker channel gains to maintain UE's fairness under near-far pairing. Denote  $\alpha_i$  as the power coefficient allocated to UE i, we applied a varied power coefficient setting according to [49], i.e.,  $\alpha_i = \frac{i}{\kappa}$  for all K UEs sharing one radio resource, where  $\kappa$  is a normalized

factor to ensure  $\sum_{i=1}^K \alpha_i = 1$ . Without loss of generality, two UEs with different channel disparities are considered under  $[\alpha_1,\alpha_2]=[\frac{1}{3},\frac{2}{3}]$ . In Fig. 12, similar results have been obtained as that in uplink transmission. It is shown that our proposed CQP receiver also has significant performance gains over the existing DLMV receiver even when the received power difference between far and near UEs is small. Moreover, the BER can be further improved by optimally allocating  $\alpha_i$  based on channel conditions.

#### VI. CONCLUSION

This paper studies robust receiver design for non-orthogonal multiple access (NOMA) with successive interference cancellation (SIC). In particular, we tackle the problems of residual interference and error propagation in SIC process caused by CSI mismatch at receiver. In order to alleviate performance loss caused by the CSI uncertainty, we develop a minimum output energy (MOE)-based receiver to recover the desired signal while rejecting inter-user interference. Unlike existing formulations that solely focus on imperfect CSI, our novel contribution utilizes forward error correction (FEC) code constraints as unique UE signatures to substantially improve robustness and reliability of receiver output. We formulate a quadratic programming optimization problem to incorporate a set of transformed FEC code constraints. For further performance enhancement, we extend the code configurations to a serial concatenation of FEC codes along with iterative detection for more accurate signal reconstruction that the SIC receiver relies on. Simulation results demonstrate that the proposed receiver achieves substantially lower error rates when compared to receivers without code constraints. Our design clearly achieves a high degree of robustness against imperfect CSI.

#### REFERENCES

- [1] F. Boccardi, R. W. Heath, A. Lozano, T. L. Marzetta, and P. Popovski, "Five disruptive technology directions for 5G," *IEEE Commun. Mag.*, vol. 52, no. 2, pp. 74–80, Feb. 2014.
- [2] Study Scenarios Requirements for Next Generation Access technol. (Release 14), document TR 38.913 V0.2.0, 3GPP, 2016.
- [3] Q. Sun, S. Han, C. L. I., and Z. Pan, "On the ergodic capacity of MIMO NOMA systems," *IEEE Wireless Commun. Lett.*, vol. 4, no. 4, pp. 405–408, Aug. 2015.
- [4] L. Dai, B. Wang, Y. Yuan, S. Han, C.-L. I, and Z. Wang, "Non-orthogonal multiple access for 5G: Solutions, challenges, opportunities, and future research trends," *IEEE Commun. Mag.*, vol. 53, no. 9, pp. 74–81, Sep. 2015.
- [5] Z. Ding et al., "Impact of user pairing on 5G nonorthogonal multipleaccess downlink transmissions," IEEE Trans. Veh. Technol., vol. 65, no. 8, pp. 6010–6023, Aug. 2016.
- [6] P. D. Diamantoulakis, K. N. Pappi, Z. Ding, and G. K. Karagiannidis, "Wireless-powered communications with non-orthogonal multiple access," *IEEE Trans. Wireless Commun.*, vol. 15, no. 12, pp. 8422–8436, Dec. 2016.
- [7] L. Lei, D. Yuan, C. K. Ho, and S. Sun, "Power and channel allocation for non-orthogonal multiple access in 5G systems: Tractability and computation," *IEEE Trans. Wireless Commun.*, vol. 15, no. 12, pp. 8580–8594, Dec. 2016.
- [8] T. L. Marzetta, "Noncooperative cellular wireless with unlimited numbers of base station antennas," *IEEE Trans. Wireless Commun.*, vol. 9, no. 11, pp. 3590–3600, Nov. 2010.
- [9] R. R. Müller, L. Cottatellucci, and M. Vehkaperä, "Blind pilot decontamination," *IEEE J. Sel. Topics Signal Process.*, vol. 8, no. 5, pp. 773–786, Oct. 2014.

- [10] J. Zhang, B. Zhang, S. Chen, X. Mu, M. El-Hajjar, and L. Hanzo, "Pilot contamination elimination for large-scale multiple-antenna aided OFDM systems," *IEEE J. Sel. Topics Signal Process.*, vol. 8, no. 5, pp. 759–772, Oct. 2014.
- [11] S. Shahbazpanahi, M. Beheshti, A. B. Gershman, M. Gharavi-Alkhansari, and K. M. Wong, "Minimum variance linear receivers for multiaccess MIMO wireless systems with space-time block coding," *IEEE Trans. Signal Process.*, vol. 52, no. 12, pp. 3306–3313, Dec. 2004.
- [12] Y. Rong, S. Shahbazpanahi, and A. B. Gershman, "Robust linear receivers for space-time block coded multiaccess MIMO systems with imperfect channel state information," *IEEE Trans. Signal Process.*, vol. 53, no. 8, pp. 3081–3090, Aug. 2005.
- [13] Y. Rong, S. A. Vorobyov, and A. B. Gershman, "Robust linear receivers for multiaccess space-time block-coded MIMO systems: A probabilistically constrained approach," *IEEE J. Sel. Areas Commun.*, vol. 24, no. 8, pp. 1560–1570, Aug. 2006.
- [14] J. Dai, K. Niu, Z. Si, C. Dong, and J. Lin, "Polar-coded nonorthogonal multiple access," *IEEE Trans. Signal Process.*, vol. 66, no. 5, pp. 1374–1389, Mar. 2018.
- [15] M. Jiang, G. Yue, N. Prasad, and S. Rangarajan, "Link adaptation in LTE-A uplink with Turbo SIC receivers and imperfect channel estimation," in *Proc. IEEE CISS*, Mar. 2011, pp. 1–6.
- [16] K. Wang, W. Wu, and Z. Ding, "Joint detection and decoding of LDPC coded distributed space-time signaling in wireless relay networks via linear programming," in *Proc. IEEE ICASSP*, May 2014, pp. 1906–1910.
- [17] K. Wang, H. Shen, W. Wu, and Z. Ding, "Joint detection and decoding in LDPC-based space-time coded MIMO-OFDM systems via linear programming," *IEEE Trans. Signal Process.*, vol. 63, no. 13, pp. 3411–3424, Jul. 2015.
- [18] K. Wang and Z. Ding, "FEC code anchored robust design of massive MIMO receivers," *IEEE Trans. Wireless Commun.*, vol. 15, no. 12, pp. 8223–8235, Dec. 2016.
- [19] K. Wang and Z. Ding, "Robust receiver design based on FEC code diversity in pilot-contaminated multi-user massive mimo systems," in Proc. IEEE ICASSP, Mar. 2016, pp. 3426–3430.
- [20] D. Tse and P. Viswanath, Fundamentals of Wireless Communication. Cambridge, U.K.: Cambridge Univ. Press, 2005.
- [21] M. A. Dangl, C. Sgraja, and J. Lindner, "An improved block equalization scheme for uncertain channel estimation," *IEEE Trans. Wireless Commun.*, vol. 6, no. 1, pp. 146–156, Jan. 2007.
- [22] G. Caire, N. Jindal, M. Kobayashi, and N. Ravindran, "Multiuser MIMO achievable rates with downlink training and channel state feedback," *IEEE Trans. Inf. Theory*, vol. 56, no. 6, pp. 2845–2866, Jun. 2010.
- [23] N. Krishnan, R. D. Yates, and N. B. Mandayam, "Uplink linear receivers for multi-cell multiuser MIMO with pilot contamination: Large system analysis," *IEEE Trans. Wireless Commun.*, vol. 13, no. 8, pp. 4360–4373, Aug. 2014.
- [24] Y. Saito, A. Benjebbour, Y. Kishiyama, and T. Nakamura, "System-level performance evaluation of downlink non-orthogonal multiple access (NOMA)," in *Proc. IEEE PIMRC*, Sep. 2013, pp. 611–615.
- [25] A. Benjebbovu, A. Li, Y. Saito, Y. Kishiyama, A. Harada, and T. Nakamura, "System-level performance of downlink NOMA for future LTE enhancements," in *Proc. IEEE Globecom Workshops*, Dec. 2013, pp. 66–70.
- [26] J. Dai, K. Niu, Z. Si, and J. Lin, "Polar coded non-orthogonal multiple access," in *Proc. IEEE ISIT*, Jul. 2016, pp. 988–992.
- [27] K. Saito, A. Benjebbour, A. Harada, Y. Kishiyama, and T. Nakamura, "Link-level performance of downlink NOMA with SIC receiver considering error vector magnitude," in *Proc. IEEE VTC Spring*, May 2015, pp. 1–5.
- [28] K. Saito, A. Benjebbour, Y. Kishiyama, Y. Okumura, and T. Nakamura, "Performance and design of SIC receiver for downlink NOMA with open-loop SU-MIMO," in *Proc. IEEE ICC Workshops*, Jun. 2015, pp. 1161–1165.
- [29] M. Honig and M. K. Tsatsanis, "Adaptive techniques for multiuser CDMA receivers," *IEEE Signal Process. Mag.*, vol. 17, no. 3, pp. 49–61, May 2000.
- [30] S. Vembu, S. Verdu, R. A. Kennedy, and W. Sethares, "Convex cost functions in blind equalization," *IEEE Trans. Signal Process.*, vol. 42, no. 8, pp. 1952–1960, Aug. 1994.
- [31] M. Honig, U. Madhow, and S. Verdu, "Blind adaptive multiuser detection," *IEEE Trans. Inf. Theory*, vol. 41, no. 4, pp. 944–960, Jul. 1995.

- [32] H. L. Van Trees, Optimum Array Processing: Part IV of Detection, Estimation, and Modulation Theory, vol. 1. Hoboken, NJ, USA: Wiley, 2002
- [33] A. B. Gershman, Y. Hua, and Q. Cheng, Robustness Issues in Adaptive Beamforming and High-Resolution Direction Finding. New York, NY, USA: Marcel Dekker, 2003.
- [34] J. Feldman, M. J. Wainwright, and D. R. Karger, "Using linear programming to decode binary linear codes," *IEEE Trans. Inf. Theory*, vol. 51, no. 3, pp. 954–972, Mar. 2005.
- [35] M. F. Flanagan, "A unified framework for linear-programming based communication receivers," *IEEE Trans. Commun.*, vol. 59, no. 12, pp. 3375–3387, Dec. 2011.
- [36] N. Jacklin and Z. Ding, "On efficient utilization of training pilots for linear equalization of QAM transmissions," *IEEE Trans. Commun.*, vol. 61, no. 12, pp. 4984–4996, Dec. 2013.
- [37] D. Bertsimas and J. N. Tsitsiklis, Introduction to Linear Optimization. Belmont, MA, USA: Athena Scientific, 1997, vol. 6.
- [38] D. J. C. MacKay, "Good error-correcting codes based on very sparse matrices," *IEEE Trans. Inf. Theory*, vol. 45, no. 2, pp. 399–431, Mar. 1999.
- [39] I. S. Reed and G. Solomon, "Polynomial codes over certain finite fields," J. Soc. Ind. Appl. Math., vol. 8, no. 2, pp. 300–304, Jun. 1960.
- [40] R. J. McEliece, The Theory of Information and Coding, vol. 3. Cambridge, U.K.: Cambridge Univ. Press, 2002.
- [41] J. G. Proakis and M. Salehi, *Digital Communications*. New York, NY, USA: McGraw-Hill, 2008.
- [42] K. Zarifi and A. B. Gershman, "Asymptotic performance analysis of blind minimum output energy receivers for large DS-CDMA systems," *IEEE Trans. Signal Process.*, vol. 56, no. 2, pp. 650–663, Feb. 2008.
- [43] B. Sklar, *Digital Communications*, vol. 2. Upper Saddle River, NJ, USA: Prentice-Hall, 2001.
- [44] A. Goldsmith, Wireless Communications. Cambridge, U.K.: Cambridge Univ. Press, 2005.
- [45] M. S. Lobo, L. Vandenberghe, S. Boyd, and H. Lebret, "Applications of second-order cone programming," *Linear Algebra Appl.*, vol. 284, nos. 1–3, pp. 193–228, Nov. 1998.
- [46] CVX: MATLAB Software for Disciplined Convex Programming. Accessed: Jul. 19, 2015. [Online]. Available: http://cvxr.com/cvx/
- [47] M. Baldi, QC-LDPC Code-Based Cryptography. New York, NY, USA: Springer, 2014.
- [48] F. Rusek *et al.*, "Scaling up MIMO: Opportunities and challenges with very large arrays," *IEEE Signal Process. Mag.*, vol. 30, no. 1, pp. 40–60, Jan. 2013.
- [49] Z. Ding, Z. Yang, P. Fan, and H. V. Poor, "On the performance of non-orthogonal multiple access in 5G systems with randomly deployed users," *IEEE Signal Process. Lett.*, vol. 21, no. 12, pp. 1501–1505, Dec. 2014.



Zhi Ding (S'88–M'90–SM'95–F'03) received the Ph.D. degree in electrical engineering from Cornell University, Ithaca, NY, USA, in 1990. From 1990 to 2000, he was a Faculty Member with Auburn University, Auburn, AL, USA, and, later, with The University of Iowa, Iowa City, IA, USA. He has held visiting positions with Australian National University, The Hong Kong University of Science and Technology, NASA Lewis Research Center, and USAF Wright Laboratory. He has active collaboration with researchers from Australia, Canada,

China, Finland, Hong Kong, Japan, South Korea, Singapore, and Taiwan. He is currently a Professor of electrical and computer engineering with the University of California at Davis, Davis, CA USA. He is a coauthor of the book *Modern Digital and Analog Communication Systems*, 5th edition, (Oxford University Press, 2019).

Dr. Ding was a member of the Technical Committee on Statistical Signal and Array Processing, and a member of the Technical Committee on Signal Processing for Communications from 1994 to 2003. He has been an active member of the IEEE, serving on technical programs of several workshops and conferences. He has served as a Steering Committee Member for the IEEE Transactions on Wireless Communications from 2007 to 2009 and as the Chair from 2009 to 2010. He was the General Chair of the 2016 IEEE International Conference on Acoustics, Speech, and Signal Processing, and the Technical Program Chair of the 2006 IEEE Globecom. He was an IEEE Distinguished Lecturer of Circuits and Systems Society from 2004 to 2006 and Communications Society from 2008 to 2009. He was an Associate Editor of the IEEE TRANSACTIONS ON SIGNAL PROCESSING from 1994 to 1997 and from 2001 to 2004, and an Associate Editor of the IEEE SIGNAL PROCESSING LETTERS from 2002 to 2005.



Kai-Ten Feng received the B.S. degree from the National Taiwan University, Taipei, Taiwan, in 1992, the M.S. degree from the University of Michigan, Ann Arbor, MI, USA, in 1996, and the Ph.D. degree from the University of California at Berkeley, Berkeley, CA, USA, in 2000.

From July 2009 to March 2010, he was a Visiting Research Fellow with the Department of Electrical and Computer Engineering, University of California at Davis, Davis, CA USA. From 2000 to 2003, he was an In-Vehicle Development Manager/Senior

Technologist with OnStar Corporation, a subsidiary of General Motors Corporation, where he worked on the design of future Telematics platforms and in-vehicle networks. Since August 2011, he has been a Full Professor with the Department of Electrical and Computer Engineering, National Chiao Tung University (NCTU), Hsinchu, Taiwan, where he was an Associate Professor from August 2007 to July 2011 and from February 2003 to July 2007, respectively. He has been serving as the Associated Dean of the Electrical and Computer Engineering College, NCTU, since February 2017. His current research interests include broadband wireless networks, cooperative and cognitive networks, smart phone and embedded system designs, wireless location technologies, and intelligent transportation systems.

Dr. Feng was a recipient of the Best Paper Award from the Spring 2006 IEEE Vehicular Technology Conference, which ranked his paper first among the 615 accepted papers, the Outstanding Youth Electrical Engineer Award from the Chinese Institute of Electrical Engineering in 2007, and the Distinguished Researcher Award from NCTU in 2008, 2010, and 2011, respectively. He has been serving as the Technical Advisor for IEEE-HKN honor society and National Academy of Engineering (NAE) Grand Challenges Scholars Program (GCSP) at NCTU since 2018. He has also served on the technical program committees in various international conferences.



**Pei-Rong Li** received the B.S. degree from the Department of Communications Engineering, Yuan Ze University, Taoyuan, Taiwan, in 2012, and the Ph.D. degree from the Institute of Communications Engineering, National Chiao Tung University (NCTU), Hsinchu, Taiwan, in 2019.

From March 2017 to November 2017, she was a Visiting Scholar with the Department of Electrical and Computer Engineering, University of California at Davis, Davis, CA, USA. She also visited the 5GIC Center, University of Surrey, U.K., from July 2018 to

August 2018. Since March 2019, she has been a Post-Doctoral Research Fellow with the Department of Electrical and Computer Engineering, NCTU. She is currently a Visiting Post-Doctoral Research Fellow with the School of Electronics and Computer Science, University of Southampton, U.K. Her research interests are in the areas of wireless communications, including radio resource management, functional splitting, and network slicing technologies for 5G networks. She is also involved in signal processing for wireless communications with special emphasis on joint design of detection and decoding.